

Optimal Design of Experiments on Riemannian Manifolds

Hang Li*

Department of Industrial and Manufacturing Engineering,
Pennsylvania State University

and

Enrique Del Castillo

Department of Industrial and Manufacturing Engineering,
Pennsylvania State University

and

George Runger

Department of Biomedical Informatics,
Arizona State University

October 18, 2021

Abstract

Traditional optimal design of experiment theory is developed on Euclidean space. In this paper, new theoretical results of optimal design of experiments on Riemannian manifolds are provided. In particular, it is shown that D-optimal and G-optimal designs are equivalent on manifolds and provide a lower bound for the maximum prediction variance. In addition, a converging algorithm that finds the optimal experimental design on manifold data is proposed. Numerical experiments demonstrate the competitive performance of the new algorithm.

*The authors gratefully acknowledge *NSF grant CMMI 1537898*

Keywords: Manifold learning, active learning, high-dimensional data analysis, regularization.

1 Introduction

Supervised learning models typically need to be trained on large amounts of labeled instances to perform well. While many modern systems can easily produce a large number of unlabeled instances at low cost, the labeling process can be very difficult, expensive or time-consuming. However, different labeled instances contain various information and contribute to the learning process in different ways. Therefore, an interesting question arises: how to choose the most informative instances to label so that one can improve learning rate of the model and reduce the labeling cost at the same time?

In statistics, the problem of selecting which instances to label is referred as *Design of Experiments* (**DOE**) (Federov (1972); Box et al. (2005); Del Castillo (2007)). DOE is a systematic method to explore the relationship between process input (or experimental “factors”) and output responses under limited resources for conducting experiments. Traditional DOE was developed for physical experiments in agricultural and industrial applications where the goal is to optimize some continuous function of the covariates. A classic theory of experimental design exists for linear statistical models that assume the response is a function of a small number of covariates (for a summary of this theory, see, e.g., Federov (1972)). In these problems, the number of covariates or “factors” of interest in an experiment is relatively small and so is the number of tests or size of the experiment, given the high experimental cost. However, with the development of modern technology, scientists and engineers frequently face different challenges arising not only from higher dimensional data but also from more complex data structures. Furthermore, in experi-

ments where the response is an image that needs to be classified or text that needs to be recognized and categorized, the dimension of each data instance is much higher than those typically dealt with in the classical DOE literature. A particular type of data complexity specially important in experiments with image and text data occurs when the problem data actually lies on an unknown manifold of much smaller dimension of the space in which it appears to reside.

The goal of this paper is to discuss a new methodology for designing optimal experimental designs that minimize the number of experimental runs for high-dimensional manifold data and at the same time acquire as much useful information about the response as possible. As far as we know, no existing work has provided a theoretical justification of optimal experimental design methods for high-dimensional manifold data. This paper contributes to the theoretical development of DOE methods on manifolds. In particular, we prove a new Equivalence Theorem for a continuous optimal design on a Riemannian manifolds, and also provide a converging algorithm for finding the optimal design.

The rest of this paper is organized as follows. In Section 2, we briefly introduce the traditional *Optimal Design of Experiment* (**ODOE**) on Euclidean space, and then explain the idea of manifold learning, in particular the *manifold regularization* model from Belkin et al. (2006). More importantly, a manifold-based ODOE scheme is discussed. In Section 3, we provide the theoretical justification of optimal experimental design and present a new equivalence theorem of ODOE on Riemannian manifolds. In Section 4, we illustrate our proposed algorithm and provide a convergence analysis. In Section 5, several numerical experiments are conducted to demonstrate the effectiveness of the proposed algorithm for finding optimal designs on manifold data. In Section 6, we conclude this paper and discuss some possible future directions.

2 Optimal Design of Experiments on Manifolds

2.1 Traditional ODOE on Euclidean Space

Consider initially a classical linear regression model

$$y = f(x, \beta) + \varepsilon = \beta^\top g(x) + \varepsilon, \quad (1)$$

where $g : \mathbb{R}^d \rightarrow \mathbb{R}^p$ is some nonlinear mapping function that maps from the input space $x \in \mathbb{R}^d$ to the feature space \mathbb{R}^p , $\beta \in \mathbb{R}^p$ is a column vector of unknown parameters, and ε is assumed to have a $N(0, \sigma^2)$ distribution. Given a sample of n design points $\{x_i\}_{i=1}^n$, if the corresponding response values $\{y_i\}_{i=1}^n$ are available, the well-known ordinary least squares estimates of the β parameters are given by:

$$\hat{\beta} = \underset{\beta \in \mathbb{R}^p}{\operatorname{argmin}} \left\{ \sum_{i=1}^n (y_i - \beta^\top g(x_i))^2 \right\} = (X^\top X)^{-1} X^\top Y \quad (2)$$

where X is a $n \times p$ design matrix with i -th row defined as $g(x_i)^\top$, and Y is a $n \times 1$ response vector. As a result, the corresponding fitted function is $\hat{f}(x) = \hat{\beta}^\top g(x)$.

Classical work on *Optimal Design of Experiments* (**ODOE**) was developed by Kiefer and Wolfowitz (1960) and summarized by Fedorov (1972). The goal of ODOE is to find an experimental design that is optimal with respect to some statistical criterion related either to the model parameter estimates or to the model predictions. For example, given the linear regression model (1), the *D-optimality* criterion minimizes the determinant of the covariance matrix of the parameter estimates $\operatorname{Var}(\hat{\beta}) = \sigma^2 (X^\top X)^{-1}$, while the *G-optimality* criterion minimizes the maximum prediction variance $\max_{i=1, \dots, n} \{ \operatorname{Var}(\hat{y}_i) \}$. These and similar criteria are called “*alphabetic optimality*” design criteria by Box and Draper (2007).

Traditional ODOE methods assume both the covariate and response data lie on an Euclidean space under the classical linear regression model (2). However, in applications to

high-dimensional image and text datasets, traditional ODOE is not applicable as it does not consider the intrinsic manifold structure these type of datasets usually have (Tenenbaum et al. (2000); Roweis and Saul (2000)).

While there have been recent attempts at applying alphabetic optimality criteria to manifold learning models (He (2010); Chen et al. (2010); Alaeddini et al. (2019)), no theoretical justification exists, as far as we know, to these methods, and no guarantees can be given for their success other than empirical experiments. A new theory for the optimal experimental designs is therefore needed that explicitly considers high-dimensional manifold data, justify existing methods if possible, and shows a principled way to develop new methods. Before we discuss the design of experiments on manifolds, first we need to introduce a manifold learning model by Belkin et al. (2006) that will be used in the sequel.

2.2 Manifold Regularization Model

In the well-known paradigm of machine learning, the process of learning is seen as using the training data $\{x_i\}_{i=1}^n$ to construct a function $f : \mathcal{X} \rightarrow \mathbb{R}$ that maps a data instance x to a label variable y . Let P be the joint distribution that generates labeled data $\{(x_i, y_i)\}_{i=1}^l \subset \mathcal{X} \times \mathbb{R}$ and $P_{\mathcal{X}}$ be the marginal distribution that generates unlabeled data $\{x_i\}_{i=l+1}^n \subset \mathcal{X} \subset \mathbb{R}^d$. In order to extend the learning of functions to nonlinear manifolds, Belkin et al. (2006) assume that the conditional distribution $P(y|x)$ varies smoothly as x moves along a manifold that supports $P_{\mathcal{X}}$. In other words, if two data points $x_1, x_2 \in \mathcal{X}$ are close as measured by an intrinsic (or geodesic) distance on this manifold, then the two probabilities of the labels, $P(y|x_1)$ and $P(y|x_2)$, will be similar. These authors developed a semi-supervised learning framework that involves solving the following double regularized

objective function:

$$\hat{f} = \operatorname{argmin}_{f \in \mathcal{H}_{\mathcal{K}}} \left\{ \sum_{i=1}^l V(x_i, y_i, f) + \lambda_A \|f\|_{\mathcal{H}_{\mathcal{K}}}^2 + \lambda_I \|f\|_I^2 \right\} \quad (3)$$

where V is a given loss function (such as squared loss $(y_i - f(x_i))^2$), $\mathcal{H}_{\mathcal{K}}$ is a *Reproducing Kernel Hilbert Space* (**RKHS**) (Aronszajn (1950)) with associated Mercer kernel \mathcal{K} , $\|f\|_{\mathcal{H}_{\mathcal{K}}}^2$ is a penalty term with the norm equipped in $\mathcal{H}_{\mathcal{K}}$ that imposes smoothness conditions in the ambient space (Wahba (1990)), and $\|f\|_I^2$ is a penalty term for non-smoothness along geodesics on the intrinsic manifold structure of $P_{\mathcal{X}}$. Moreover, λ_A and λ_I are two regularization parameters that control the amount of penalization in the ambient space and in the intrinsic manifold that supports $P_{\mathcal{X}}$, respectively. Some other work in recent literature can be explained as a particular case of this general framework. For example, the spatial regression model proposed by Ettinger et al. (2016) can be seen as the manifold regularization model (3) without the ambient space regularization. There are also different work about nonparametric regression models on manifolds (Cheng and Wu (2013); Marzio et al. (2014); Lin et al. (2017)), but in this paper we focus on the manifold regularization model from Belkin et al. (2006).

Intuitively, the choice of $\|f\|_I^2$ should be a smoothness penalty corresponding to the probability distribution $P_{\mathcal{X}}$. However, in most real-world applications $P_{\mathcal{X}}$ is not known, and therefore empirical estimates of the marginal distribution must be used. Considerable research has been devoted to the case when $P_{\mathcal{X}}$ is supported on a compact manifold $\mathcal{M} \subset \mathbb{R}^d$ (Roweis and Saul (2000); Tenenbaum et al. (2000); Belkin and Niyogi (2003); Donoho and Grimes (2003); Coifman et al. (2005)). Under this assumption, it can be shown that problem (3) can be reduced to

$$\hat{f} = \operatorname{argmin}_{f \in \mathcal{H}_{\mathcal{K}}} \left\{ \sum_{i=1}^l V(x_i, y_i, f) + \lambda_A \|f\|_{\mathcal{H}_{\mathcal{K}}}^2 + \lambda_I \mathbf{f}^{\top} L \mathbf{f} \right\} \quad (4)$$

where $\mathbf{f} = [f(x_1), \dots, f(x_n)]^\top$ and L is the Laplacian matrix associated with the data adjacency graph \mathcal{G} that is constructed on all the labeled and the unlabeled data points $\{x_i\}_{i=1}^n$. In particular, the graph Laplacian L approximates the *Laplace-Beltrami* operator acting on the continuous Riemannian manifold \mathcal{M} (see Belkin (2003); Lafon (2004); Belkin and Niyogi (2005); Coifman et al. (2005); Hein et al. (2005)). In this way, Belkin et al. provide a theoretical justification to the common trick in manifold learning of using a graph and geodesic distances on the graph as an approximate representation of the manifold \mathcal{M} , providing a precise sense in which the graph approaches \mathcal{M} as the number of data points gets denser. This way, the term $\mathbf{f}^\top L \mathbf{f}$ serves as an approximation for $\|f\|_L^2$, and enforces the penalization on the lack of smoothness of f as it varies between adjacent points in the graph \mathcal{G} .

In addition, Belkin et al. (2006) proceed to prove a representer theorem (similar to the theory of splines in Wahba (1990)), which shows how the solution of the infinite dimensional problem (4) can be represented in terms of a finite sum over the labeled and unlabeled points:

$$f(x) = \sum_{i=1}^n \alpha_i \mathcal{K}(x_i, x) \quad (5)$$

where $\mathcal{K}(\cdot, \cdot)$ is the Mercer kernel associated with the ambient space $\mathcal{H}_{\mathcal{K}}$. More details about the manifold regularized model can be found in Belkin et al. (2006).

2.3 Regularized ODOE on Manifolds

As far as we know, the first discussion of regularized ODOE comes from Vuchkov (1977), who proposed a ridge-type procedure for ODOE based on the ridge regression estimator:

$$\hat{\beta}_{\text{ridge}} = \underset{\beta \in \mathbb{R}^p}{\operatorname{argmin}} \left\{ \sum_{i=1}^l (y_i - \beta^\top g(x_i))^2 + \lambda_{\text{ridge}} \|\beta\|^2 \right\} \quad (6)$$

Vuchkov's motivation was to use the ridge estimator to solve the singular or ill-conditional problems that might exist in the sequential D-optimal design algorithm when the number of design points is smaller than the number of parameters to estimate. The ridge solution (6) can be seen as a particular case of the more general learning problem (4) where V is a squared-loss function, and the RKHS \mathcal{H}_K is equipped with a L^2 -norm and the manifold regularization parameter $\lambda_I = 0$.

To discuss the optimal experimental design for the general manifold regularization model (4), we first need to clarify some notation. Without loss of generality, assume a sequential experimental design generation, starting with no labeled data at the beginning of the sequence. Let $\{z_i\}_{i=1}^k \subset \{x_i\}_{i=1}^n$ be the set of points that has been labeled at the k -th iteration, and $\mathbf{y} = (y_1, \dots, y_k)^\top$ be the corresponding label vector. Given a square loss function, the manifold regularization model (4) becomes the *Laplacian Regularized Least Squares* (**LapRLS**) problem:

$$\hat{f} = \underset{f \in \mathcal{H}_K}{\operatorname{argmin}} \left\{ \sum_{i=1}^k (y_i - f(z_i))^2 + \lambda_A \|f\|_{\mathcal{H}_K}^2 + \lambda_I \mathbf{f}^\top L \mathbf{f} \right\}. \quad (7)$$

Substituting the representer theorem (5) to (7), we get a convex differentiable objective function with respect to α :

$$\hat{\alpha} = \underset{\alpha \in \mathbb{R}^n}{\operatorname{argmin}} \left\{ (\mathbf{y} - K_{XZ}^\top \alpha)^\top (\mathbf{y} - K_{XZ}^\top \alpha) + \lambda_A \alpha^\top K \alpha + \lambda_I \alpha^\top K L K \alpha \right\}, \quad (8)$$

where K_{XZ} and K are the Gram matrix defined by

$$K_{XZ} = \begin{bmatrix} \mathcal{K}(x_1, z_1) & \dots & \mathcal{K}(x_1, z_k) \\ \vdots & \ddots & \vdots \\ \mathcal{K}(x_n, z_1) & \dots & \mathcal{K}(x_n, z_k) \end{bmatrix}_{n \times k}, \quad K_{XX} = \begin{bmatrix} \mathcal{K}(x_1, x_1) & \dots & \mathcal{K}(x_1, x_n) \\ \vdots & \ddots & \vdots \\ \mathcal{K}(x_n, x_1) & \dots & \mathcal{K}(x_n, x_n) \end{bmatrix}_{n \times n},$$

and \mathcal{K} is the kernel embedded in the RKHS \mathcal{H}_K . Taking a derivative of (8) with respect to α and making it equal to 0, we arrive at the following expression:

$$\hat{\alpha} = (K_{XZ}K_{XZ}^\top + \lambda_A K + \lambda_I K L K)^{-1} K_{XZ} \mathbf{y} \quad (9)$$

Consider a linear regression model form (1) and a linear kernel for \mathcal{H}_K , the regression parameters β can be estimated by

$$\hat{\beta} = X^\top \hat{\alpha} = X^\top (X Z_k^\top Z_k X^\top + \lambda_A X X^\top + \lambda_I X X^\top L X X^\top)^{-1} X Z_k^\top \mathbf{y} \quad (10)$$

where

$$Z_k = \begin{bmatrix} g(z_1)^\top \\ \vdots \\ g(z_k)^\top \end{bmatrix}, \quad X = \begin{bmatrix} g(x_1)^\top \\ \vdots \\ g(x_n)^\top \end{bmatrix}, \quad \mathbf{y} = \begin{bmatrix} y_1 \\ \vdots \\ y_k \end{bmatrix}. \quad (11)$$

By some simple linear algebra (a formal proof is provided in the Appendix), the estimated parameters $\hat{\beta}$ (10) can be simplified to

$$\hat{\beta} = (Z_k^\top Z_k + \lambda_A I_p + \lambda_I X^\top L X)^{-1} Z_k^\top \mathbf{y} \quad (12)$$

He (2010) demonstrated that the covariance matrix of (12) can be approximated as:

$$\text{Cov}(\hat{\beta}) \approx \sigma^2 (Z_k^\top Z_k + \lambda_A I_p + \lambda_I X^\top L X)^{-1}. \quad (13)$$

The determinant of covariance matrix (13) is the statistical criterion we will minimize to obtain a D-optimal design. Before we discuss the optimal design algorithm, first we will provide some theoretical justification of ODOE on Riemannian manifolds in the following section.

3 Theoretical Results

When the determinant of $Z_k^\top Z_k + \lambda_A I_p + \lambda_I X^\top L X$ is maximized, one obtains a so-called *D-optimal* experimental design. In Euclidean space, “continuous” or “exact” optimal design theory (which considers the proportion of experimental tests allocated to different locations over the space) indicates the equivalence between the D-optimality criteria and the so-called *G-optimality* criteria, where the maximum prediction variance is minimized, as stated by the celebrated *Kiefer-Wolfowitz (KW)* theorem (Kiefer and Wolfowitz (1960); Kiefer (1974)). In analogy with the KW theorem, we aim to develop a new equivalence result for optimal experimental design based on the manifold regularization model (4), which can then be used for designing an experiment on a Riemannian manifold.

Assume there is an infinite number of points x that are uniformly distributed on a Riemannian manifold \mathcal{M} . Let ϵ be a continuous design on \mathcal{M} . For any continuous design ϵ , based on the *Carathéodory Theorem*, it’s known that ϵ can be represented as

$$\epsilon = \left\{ \begin{array}{c} z_1, z_2, \dots, z_{n_0} \\ q_1, q_2, \dots, q_{n_0} \end{array} \right\}, \text{ where } \sum_{i=1}^{n_0} q_i = 1. \quad (14)$$

For any ϵ , the corresponding information matrix of LapRLS model is defined as

$$M_{Lap}(\epsilon) = \int_{z \in \mathcal{X}} \xi(z) g(z) g(z)^\top dz + \lambda_A I_p + \lambda_I \int_{x \in \mathcal{M}} g(x) \Delta_{\mathcal{M}} g(x)^\top d\mu, \quad (15)$$

where ξ is a probability measure of design ϵ on the experimental region $\mathcal{X} \subseteq \mathcal{M} \subset \mathbb{R}^p$, $\Delta_{\mathcal{M}}$ is the *Laplace-Beltrami* operator on \mathcal{M} , and μ is the uniform measure on \mathcal{M} . Note that the last two terms in (15) are independent of the design ϵ , thus for simplicity, define

$$C = \lambda_A I_p + \lambda_I \int_{x \in \mathcal{M}} g(x) \Delta_{\mathcal{M}} g(x)^\top d\mu. \quad (16)$$

Then (15) can be written as

$$M_{Lap}(\epsilon) = \int_{z \in \mathcal{X}} \xi(z) g(z) g(z)^\top dz + C. \quad (17)$$

Based on the parameters estimates (12), for a given continuous design ϵ , the prediction variance at a test point z is

$$d(z, \epsilon) = \text{Var} \left[\hat{\beta}^\top g(z) \right] = g(z)^\top \text{Cov}(\hat{\beta}) g(z) = \sigma^2 g(z)^\top M_{Lap}^{-1}(\epsilon) g(z) \quad (18)$$

As it can be seen, under the LapRLS model one can obtain a D-optimal design by maximizing the determinant of $M_{Lap}(\epsilon)$ and a G-optimal design by minimizing $\max_{z \in \mathcal{X}} d(z, \epsilon)$. Similarly to the optimal design of experiments in Euclidean space, we prove next an equivalence theorem on Riemannian manifolds that shows how the D and G optimality criteria lead to the same optimal design. Before the equivalence theorem is discussed, we need to prove some auxiliary results. The proofs of these proposition are provided in the Appendix.

Proposition 1. *Let ϵ_1 and ϵ_2 be two designs with the corresponding information matrices $M_{Lap}(\epsilon_1)$ and $M_{Lap}(\epsilon_2)$. Then*

$$M_{Lap}(\epsilon_3) = (1 - \alpha) M_{Lap}(\epsilon_1) + \alpha M_{Lap}(\epsilon_2), \quad (19)$$

where $M_{Lap}(\epsilon_3)$ is the information matrix of the design

$$\epsilon_3 = (1 - \alpha) \epsilon_1 + \alpha \epsilon_2. \quad (20)$$

Proposition 2. *Let ϵ_1 and ϵ_2 be two designs with the corresponding information matrices $M_{Lap}(\epsilon_1)$ and $M_{Lap}(\epsilon_2)$. Then*

$$\frac{d \log |M_{Lap}(\epsilon_3)|}{d\alpha} = \text{Tr} \left\{ M_{Lap}^{-1}(\epsilon_3) [M_{Lap}(\epsilon_2) - M_{Lap}(\epsilon_1)] \right\}, \quad (21)$$

where $M_{Lap}(\epsilon_3)$ is the information matrix of the design

$$\epsilon_3 = (1 - \alpha)\epsilon_1 + \alpha\epsilon_2. \quad (22)$$

Proposition 3. *For any continuous design ϵ ,*

1.

$$\int_{z \in \mathcal{X}} d(z, \epsilon) \xi(z) dz = p - \text{Tr} \left\{ M_{Lap}^{-1}(\epsilon) C \right\} \quad (23)$$

2.

$$\max_{z \in \mathcal{X}} d(z, \epsilon) \geq p - \text{Tr} \left\{ M_{Lap}^{-1}(\epsilon) C \right\} \quad (24)$$

Proposition 4. *The function $\log |M_{Lap}(\epsilon)|$ is a strictly concave function.*

Based on Propositions 1-4, we can now prove the equivalence theorem for the LapRLS model. In summary, the following theorem demonstrates that the D-optimal design and G-optimal design are equivalent on the Riemannian manifold \mathcal{M} . It also provides the theoretical value of maximum prediction variance of the LapRLS model when the D/G optimal design is achieved.

Theorem 1 (Equivalence Theorem). *The following statements are equivalent:*

1. *the design ϵ^* maximizes $\det(M_{Lap}(\epsilon))$*

2. *the design ϵ^* minimizes $\max_{z \in \mathcal{X}} d(z, \epsilon)$*

$$3. \max_{z \in \mathcal{X}} d(z, \epsilon^*) = p - \text{Tr} \left\{ M_{Lap}^{-1}(\epsilon^*) C \right\}$$

Proof

(1) **1** \Rightarrow **2**

Let ϵ^* be the design that maximizes $|M_{Lap}(\epsilon)|$ and define $\tilde{\epsilon} = (1 - \alpha)\epsilon^* + \alpha\epsilon$, where ϵ is some arbitrary design. According to Proposition 2, we have that

$$\frac{d \log |M_{Lap}(\tilde{\epsilon})|}{d\alpha} = \text{Tr} \left\{ M_{Lap}^{-1}(\tilde{\epsilon}) [M_{Lap}(\epsilon) - M_{Lap}(\epsilon^*)] \right\} \quad (25)$$

When $\alpha = 0$, we have $\tilde{\epsilon} = \epsilon^*$. Thus

$$\left. \frac{d \log |M_{Lap}(\tilde{\epsilon})|}{d\alpha} \right|_{\alpha=0} = \text{Tr} \left\{ M_{Lap}^{-1}(\epsilon^*) [M_{Lap}(\epsilon) - M_{Lap}(\epsilon^*)] \right\} \quad (26)$$

$$= \text{Tr} \left\{ M_{Lap}^{-1}(\epsilon^*) M_{Lap}(\epsilon) \right\} - \text{Tr}(I_p) \quad (27)$$

$$= \text{Tr} \left\{ M_{Lap}^{-1}(\epsilon^*) M_{Lap}(\epsilon) \right\} - p \quad (28)$$

Since ϵ^* is the maximal solution, then

$$\text{Tr} \left\{ M_{Lap}^{-1}(\epsilon^*) M_{Lap}(\epsilon) \right\} - p \leq 0. \quad (29)$$

Without loss of generality, assume the design ϵ has only one instance $z \in \mathcal{X}$. Then we have

$$M_{Lap}(\epsilon) = g(z)g(z)^\top + C \quad (30)$$

and

$$\begin{aligned} \text{Tr} \left\{ M_{Lap}^{-1}(\epsilon^*) [g(z)g(z)^\top + C] \right\} - p &= \text{Tr} \left\{ M_{Lap}^{-1}(\epsilon^*) g(z)g(z)^\top \right\} + \text{Tr} \left\{ M_{Lap}^{-1}(\epsilon^*) C \right\} - p \\ &= d(z, \epsilon^*) + \text{Tr} \left\{ M_{Lap}^{-1}(\epsilon^*) C \right\} - p \\ &\leq 0 \end{aligned}$$

Thus

$$d(z, \epsilon^*) \leq p - \text{Tr} \left\{ M_{Lap}^{-1}(\epsilon^*) C \right\} \quad (31)$$

In addition, based on Proposition 3, we have

$$\max_{z \in \mathcal{X}} d(z, \epsilon^*) \geq p - \text{Tr} \left\{ M_{Lap}^{-1}(\epsilon^*) C \right\} \quad (32)$$

Combining (31) and (32), we can conclude that the D-optimal design ϵ^* minimizes $\max_{z \in \mathcal{X}} d(z, \epsilon)$. ■

(2) 2 \Rightarrow 1

Let ϵ^* be the design that minimizes $\max_{z \in \mathcal{X}} d(z, \epsilon)$, but assume it is not D-optimal. Based on Proposition 4, we know there must exist a design ϵ such that:

$$\left. \frac{d \log |(1 - \alpha) M_{Lap}(\epsilon^*) + \alpha M_{Lap}(\epsilon)|}{d\alpha} \right|_{\alpha=0} = \text{Tr} \left\{ M_{Lap}^{-1}(\epsilon^*) M_{Lap}(\epsilon) \right\} - p > 0 \quad (33)$$

where

$$M_{Lap}(\epsilon) = \int_{z \in \mathcal{X}} \xi(z) g(z) g(z)^\top dz + C. \quad (34)$$

Then

$$\begin{aligned} & \text{Tr} \left\{ M_{Lap}^{-1}(\epsilon^*) M_{Lap}(\epsilon) \right\} - p \\ &= \text{Tr} \left\{ M_{Lap}^{-1}(\epsilon^*) \left[\int_{z \in \mathcal{X}} \xi(z) g(z) g(z)^\top dz + C \right] \right\} - p \\ &= \text{Tr} \left\{ M_{Lap}^{-1}(\epsilon^*) \int_{z \in \mathcal{X}} \xi(z) g(z) g(z)^\top dz \right\} + \text{Tr} \left\{ M_{Lap}^{-1}(\epsilon^*) C \right\} - p \\ &= \text{Tr} \left\{ \int_{z \in \mathcal{X}} M_{Lap}^{-1}(\epsilon^*) \xi(z) g(z) g(z)^\top dz \right\} + \text{Tr} \left\{ M_{Lap}^{-1}(\epsilon^*) C \right\} - p \\ &= \int_{z \in \mathcal{X}} \xi(z) \text{Tr} \left\{ M_{Lap}^{-1}(\epsilon^*) g(z) g(z)^\top \right\} dz + \text{Tr} \left\{ M_{Lap}^{-1}(\epsilon^*) C \right\} - p \\ &= \int_{z \in \mathcal{X}} \xi(z) \text{Tr} \left\{ g(z)^\top M_{Lap}^{-1}(\epsilon^*) g(z) \right\} dz + \text{Tr} \left\{ M_{Lap}^{-1}(\epsilon^*) C \right\} - p \\ &= \int_{z \in \mathcal{X}} \xi(z) d(z, \epsilon^*) dz + \text{Tr} \left\{ M_{Lap}^{-1}(\epsilon^*) C \right\} - p \end{aligned}$$

Since ϵ^* is the design that minimizes $\max_{z \in \mathcal{X}} d(z, \epsilon)$, by Proposition 3, we have

$$\max_{z \in \mathcal{X}} d(z, \epsilon^*) = p - \text{Tr} \left\{ M_{Lap}^{-1}(\epsilon) C \right\} \quad (35)$$

Thus, for any $z \in \mathcal{X}$,

$$d(z, \epsilon^*) \leq p - \text{Tr} \left\{ M_{Lap}^{-1}(\epsilon^*) C \right\} \quad (36)$$

Then

$$\int_{z \in \mathcal{X}} \xi(z) d(z, \epsilon^*) dz \leq \int_{z \in \mathcal{X}} \xi(z) \left(p - \text{Tr} \left\{ M_{Lap}^{-1}(\epsilon^*) C \right\} \right) dz \quad (37)$$

$$= \left(p - \text{Tr} \left\{ M_{Lap}^{-1}(\epsilon^*) C \right\} \right) \int_{z \in \mathcal{X}} \xi(z) dz \quad (38)$$

$$= p - \text{Tr} \left\{ M_{Lap}^{-1}(\epsilon^*) C \right\} \quad (39)$$

Therefore, we have

$$\begin{aligned} \text{Tr} \left\{ M_{Lap}^{-1}(\epsilon^*) M_{Lap}(\epsilon) \right\} - p &= \int_{z \in \mathcal{X}} \xi(z) d(z, \epsilon^*) dz + \text{Tr} \left\{ M_{Lap}^{-1}(\epsilon^*) C \right\} - p \\ &\leq p - \text{Tr} \left\{ M_{Lap}^{-1}(\epsilon^*) C \right\} + \text{Tr} \left\{ M_{Lap}^{-1}(\epsilon^*) C \right\} - p \\ &= 0. \end{aligned}$$

This contradicts with (33). Therefore, the design ϵ^* is also D-optimal. ■

(3) 1 \Rightarrow 3

Let ϵ^* be the D-optimal design. From the previous proof, in particular Equation (31), we know that

$$\max_{z \in \mathcal{X}} d(z, \epsilon^*) = p - \text{Tr} \left\{ M_{Lap}^{-1}(\epsilon) C \right\}. \quad (40)$$

■

(4) 3 \Rightarrow 1

Let ϵ^* be the design such that

$$\max_{z \in \mathcal{X}} d(z, \epsilon^*) = p - \text{Tr} \left\{ M_{Lap}^{-1}(\epsilon) C \right\}. \quad (41)$$

Then, for any $z \in \mathcal{X}$,

$$d(z, \epsilon^*) + \text{Tr} \left\{ M_{Lap}^{-1}(\epsilon^*) C \right\} - p \leq 0. \quad (42)$$

Based on the previous proof, we know that equation (42) implies that there is no improving direction for the D-optimal criteria. Thus ϵ^* is the D-optimal design.

■

(5) Since $1 \Leftrightarrow 2$, $1 \Leftrightarrow 3$, then **2 \Leftrightarrow 3** and the equivalence theoreme is proved.

■

Different from the classical equivalence theorem on Euclidean space, Theorem 1 demonstrates the equivalence of D-optimal design and G-optimal design on the Riemannian manifold. In addition, for any given design ϵ , Equation (24) provides a new lower bound for the maximum prediction variance. Theorem 1 shows that this lower bound (24) can be achieved at the D/G optimal design ϵ^* . Therefore, Theorem 1 also provides a theoretical justification that the optimal D/G design ϵ^* would minimize the maximum prediction variance of the model.

4 Proposed Algorithm and Convergence Analysis

Before we discuss our proposed algorithm for finding optimal experimental design on manifolds, some auxiliary results need to be derived.

Proposition 5. Let $M_{Lap}(\epsilon_k)$ be the information matrix of the design ϵ_k at k -th iteration. Let $M_{Lap}(\epsilon(z))$ be the information matrix of the design concentrated at one single point z . Given $\epsilon_{k+1} = (1 - \alpha)\epsilon_k + \alpha\epsilon(z)$, then

$$|M_{Lap}(\epsilon_{k+1})| = (1 - \alpha)^p |M_{Lap}(\epsilon_k)| \left[1 + \frac{\alpha}{1 - \alpha} d(z, \epsilon_k) + \frac{\alpha}{1 - \alpha} \text{Tr}(M_{Lap}^{-1}(\epsilon_k)C) \right] \quad (43)$$

Proposition 6. Let $M_{Lap}(\epsilon_k)$ be the information matrix of the design ϵ_k at k -th iteration. Construct the design ϵ_{k+1} at $(k + 1)$ -th iteration as

$$\epsilon_{k+1} = (1 - \alpha_k)\epsilon_k + \alpha_k\epsilon(z_{k+1}) \quad (44)$$

where

$$0 \leq \alpha_k \leq \frac{d(z_{k+1}, \epsilon_k) - (p - \text{Tr}(M_{Lap}^{-1}(\epsilon_k)C))}{p[d(z_{k+1}, \epsilon_k) - (1 - \text{Tr}(M_{Lap}^{-1}(\epsilon_k)C))]}, \quad z_{k+1} = \underset{z \in \mathcal{X}}{\text{argmax}} d(z, \epsilon_k). \quad (45)$$

Then the resulting sequence $\left\{ |M_{Lap}(\epsilon_k)| \right\}_k$ is non-decreasing.

Based on Proposition 5 and 6, we propose a new algorithm to find the D-G optimal experimental design on a manifold, as shown in Algorithm 1. Note how after obtaining an optimal design for the data to be labeled, and obtaining the corresponding labels, we use both labeled *and* unlabeled instances to train the manifold regularized model.

We next provide a convergence analysis of the proposed algorithm.

Theorem 2 (Convergence Theorem). The iterative procedure in Algorithm 1 converges to the D-optimal design ϵ^* ,

$$\lim_{k \rightarrow \infty} |M_{Lap}(\epsilon_k)| = |M_{Lap}(\epsilon^*)| \quad (50)$$

Algorithm 1 Optimal Design of Experiments on Manifolds (**ODOEM**)

Input: Some initial design ϵ_k ,

$$\epsilon_k = \left\{ \begin{array}{c} z_1, z_2, \dots, z_k \\ q_1, q_2, \dots, q_k \end{array} \right\}, \text{ where } \sum_{i=1}^k q_i = 1$$

Compute the information matrix

$$M_{Lap}(\epsilon_k) = \sum_{i=1}^k q_i g(z_i) g(z_i)^\top + C \quad (46)$$

while optimal design is not achieved **do**

1. Find z_{k+1} s.t.

$$z_{k+1} = \underset{z \in \mathcal{X}}{\operatorname{argmax}} d(z, \epsilon_k) \quad (47)$$

2. Update the design

$$\epsilon_{k+1} = (1 - \alpha_k) \epsilon_k + \alpha_k \epsilon(z_{k+1}) \quad (48)$$

where α_k is a user choice that satisfies

$$0 \leq \alpha_k \leq \frac{d(z_{k+1}, \epsilon_k) - [p - \operatorname{Tr}(M_{Lap}^{-1}(\epsilon_k)C)]}{p\{d(z_{k+1}, \epsilon_k) - [1 - \operatorname{Tr}(M_{Lap}^{-1}(\epsilon_k)C)]\}} \quad (49)$$

3. Compute the information matrix $M_{Lap}(\epsilon_{k+1})$, set $k = k + 1$ and repeat step 1-3.

end while

Output: Optimal Design on manifolds.

Proof

Let the design ϵ_0 not be D-optimal. Based on Proposition 6, we have

$$|M_{Lap}(\epsilon_0)| < |M_{Lap}(\epsilon_1)| \leq \dots \leq |M_{Lap}(\epsilon_k)| \leq |M_{Lap}(\epsilon^*)| \quad (51)$$

It is known that any bounded monotone sequence converges. Thus the sequence $|M_{Lap}(\epsilon_0)|, |M_{Lap}(\epsilon_1)|, \dots, |M_{Lap}(\epsilon_k)|$ converges to some limit $|M_{Lap}(\hat{\epsilon})|$. Next we need to show

$$|M_{Lap}(\hat{\epsilon})| = |M_{Lap}(\epsilon^*)| \quad (52)$$

The proof proceeds by contradiction. Assume

$$|M_{Lap}(\hat{\epsilon})| < |M_{Lap}(\epsilon^*)| \quad (53)$$

By the convergence of the sequence $|M_{Lap}(\epsilon_0)|, |M_{Lap}(\epsilon_1)|, \dots, |M_{Lap}(\epsilon_k)|$, we know that, for $\forall \eta > 0$, there $\exists k_0 \in \mathbb{N}$ s.t.

$$|M_{Lap}(\epsilon_{k+1})| - |M_{Lap}(\epsilon_k)| < \eta \text{ for } \forall k > k_0 \quad (54)$$

Based on Proposition 5, we have

$$(1 - \alpha_k)^p \left(1 + \frac{\alpha_k}{1 - \alpha_k} d(z_{k+1}, \epsilon_k) + \frac{\alpha_k}{1 - \alpha_k} \text{Tr}(M_{Lap}^{-1}(\epsilon_k)C) \right) |M_{Lap}(\epsilon_k)| - |M_{Lap}(\epsilon_k)| < \eta$$

Then,

$$(1 - \alpha_k)^p \left(1 + \frac{\alpha_k}{1 - \alpha_k} [d(z_{k+1}, \epsilon_k) + \text{Tr}(M_{Lap}^{-1}(\epsilon_k)C)] \right) < 1 + \eta |M_{Lap}(\epsilon_k)|^{-1} \quad (55)$$

Define $\tau_k = d(z_{k+1}, \epsilon_k) - [p - \text{Tr}(M_{Lap}^{-1}(\epsilon_k)C)]$, then we can rewrite (55) as

$$(1 - \alpha_k)^p \left(1 + \frac{\alpha_k}{1 - \alpha_k} [\tau_k + p] \right) < 1 + \eta |M_{Lap}(\epsilon_k)|^{-1} \quad (56)$$

Define a function $T(\tau_k, \alpha_k)$ as

$$T(\tau_k, \alpha_k) = (1 - \alpha_k)^p \left(1 + \frac{\alpha_k}{1 - \alpha_k} [\tau_k + p] \right) \quad (57)$$

Then

$$\frac{\partial T}{\partial \tau_k} = (1 - \alpha_k)^p \frac{\alpha_k}{1 - \alpha_k} \quad (58)$$

Clearly, $\frac{\partial T}{\partial \tau_k} > 0$ for $0 \leq \alpha_k < 1$. Thus, for a given α_k , $T(\tau_k, \alpha_k)$ is an increasing function with respect to τ_k . On the other hand,

$$\frac{\partial T}{\partial \alpha_k} = -p(1 - \alpha_k)^{p-1} \left(1 + \frac{\alpha_k}{1 - \alpha_k} [\tau_k + p] \right) + (1 - \alpha_k)^p [\tau_k + p] \frac{1}{(1 - \alpha_k)^2} \quad (59)$$

Let $\frac{\partial T}{\partial \alpha_k} \geq 0$, we have

$$(1 - \alpha_k)^{p-2} [\tau_k + p] \geq p(1 - \alpha_k)^{p-1} \left(1 + \frac{\alpha_k}{1 - \alpha_k} [\tau_k + p] \right) \quad (60)$$

$$\tau_k + p \geq p(1 - \alpha_k) + p(\tau_k + p)\alpha_k \quad (61)$$

$$\tau_k + p \geq p - p\alpha_k + p\tau_k\alpha_k + p^2\alpha_k \quad (62)$$

$$\tau_k \geq \alpha_k(p^2 + p\tau_k - p) \quad (63)$$

$$\alpha_k \leq \frac{\tau_k}{p(p + \tau_k - 1)} \quad (64)$$

Thus, for $0 \leq \alpha_k \leq \frac{\tau_k}{p(p + \tau_k - 1)}$ and a given τ_k , $T(\tau_k, \alpha_k)$ is an increasing function. In particular, plug in the formula of τ_k , we have

$$\frac{\tau_k}{p(p + \tau_k - 1)} = \frac{d(z_{k+1}, \epsilon_k) - [p - \text{Tr}(M_{Lap}^{-1}(\epsilon_k)C)]}{p(d(z_{k+1}, \epsilon_k) - [1 - \text{Tr}(M_{Lap}^{-1}(\epsilon_k)C)]). \quad (65)$$

Notice that $0 \leq \alpha_k \leq \frac{\tau_k}{p(p + \tau_k - 1)}$ is the same choice of α in the proposed algorithm.

In addition, based on Equation (57), it can be seen that for any $0 < \alpha_k < \frac{\tau_k}{p(p + \tau_k - 1)}$ and $\tau_k > 0$, we have $T(\tau_k, \alpha_k) > 1$. Note that η is an arbitrary positive number in equation

(56), which implies τ_k need to be an infinitely small positive number to satisfy equation (56), i.e. given $\forall \zeta > 0$, there $\exists \tilde{k}(\zeta) \in \mathbb{N}$ s.t.

$$\tau_k = d(z_{k+1}, \epsilon_k) - [p - \text{Tr}(M_{Lap}^{-1}(\epsilon_k)C)] < \zeta \text{ for } k > \tilde{k}(\zeta) \quad (66)$$

However, based on the assumption (53) and the Theorem 1, we have that

$$d(z_{k+1}, \epsilon_k) - [p - \text{Tr}(M_{Lap}^{-1}(\epsilon_k)C)] \geq \delta_k > 0 \text{ for } \forall k. \quad (67)$$

Choosing $\zeta < \delta_k$, we have a contradiction, and therefore, the convergence theorem is proved. ■

From the derivation of Algorithm 1, it is not difficult to notice that ODOEM is a model-dependent design. The corresponding manifold regularization model (7) need to be trained after a desired number of instances is labeled. As it is shown before, Algorithm 1 is a converging algorithm on a continuous design space. However, sometimes the experimental design space is not continuous and only a set of candidate points is available. For a discrete design space with a set of candidate points, one can evaluate each candidate point and choose the point with maximum prediction variance. The resulting sequence of $|M_{Lap}(\epsilon_k)|$ is still non-decreasing, since

$$\begin{aligned} |M_{Lap}(\epsilon_k) + g(z_{k+1})g(z_{k+1})^\top| &= |M_{Lap}(\epsilon_k)[1 + g(z_{k+1})^\top M_{Lap}^{-1}(\epsilon_k)g(z_{k+1})]| \\ &\geq |M_{Lap}(\epsilon_k)| \end{aligned}$$

where $z_{k+1} = \underset{z \in \mathcal{X} \setminus Z_k}{\text{argmax}} d(z, \epsilon_k) = \underset{z \in \mathcal{X} \setminus Z_k}{\text{argmax}} g(z)^\top M_{Lap}^{-1}(\epsilon_k)g(z)$.

5 Numerical Results

To illustrate the empirical performance of the proposed ODOEM algorithm in practice, we consider its application to both synthetic datasets, low dimensional manifold datasets that

permit straightforward visualization of the resulting designs, and also its application to the high dimensional real-world image datasets.

5.1 Synthetic Datasets

In this section, we generated four different two-dimensional manifold datasets: data on a Torus, on a Möbius Strip, on a figure “8” immersion of a Klein bottle and on a classic Klein bottle. Each of the first three datasets contains 400 instances and the last dataset contains 1600 instances. For all four datasets, we plot these two-dimensional manifolds in a three-dimensional Euclidean space, as shown in Figure 1-8. The colors on these manifolds represent the corresponding response values $\{y_i\}_{i=1}^n$ (or their estimates based on different experimental designs), which were defined by

$$y = \sin(u) + \sin^2(u) + \cos^2(v) \quad (68)$$

where $u \in [0, 2\pi)$ and $v \in [0, 2\pi)$. The red numbers on the manifolds represent the sequence of labeled instances by different design algorithms.

In order to show the improvement provided by using the ODOEM algorithm, we compare it with a classical D-optimal design algorithm on a kernel regression model, which does not consider the manifold structure. For both of the learning models, we choose a RBF kernel and set the range parameter to be 0.01. In addition, we choose $\lambda_A = 0.01$ in both models for numerical stability, and $\lambda_I = -\ln(k/n)$ in ODOEM (a discussion of the choice of λ_I is provided in the Appendix).

For some real-world applications, the data may not strictly lie on a given manifold due to noise. In order to explore the robustness of the ODOEM algorithm to noise, we also let the four synthetic datasets fluctuate around their manifolds by adding noise to $\{x_i\}_{i=1}^n$. In

other words, for each of the four manifolds, we investigate both of the case when the data $\{x_i\}_{i=1}^n$ lie exactly on the given manifold and the case when $\{x_i\}_{i=1}^n$ are not exactly on the manifold.

The results are shown in Figure 1-4. As it can be seen, on all four synthetic datasets, ODOEM performs much better than kernel regression D-optimal Design in terms of instance selection and function fitting, under both of the case with noises and the case without noises.

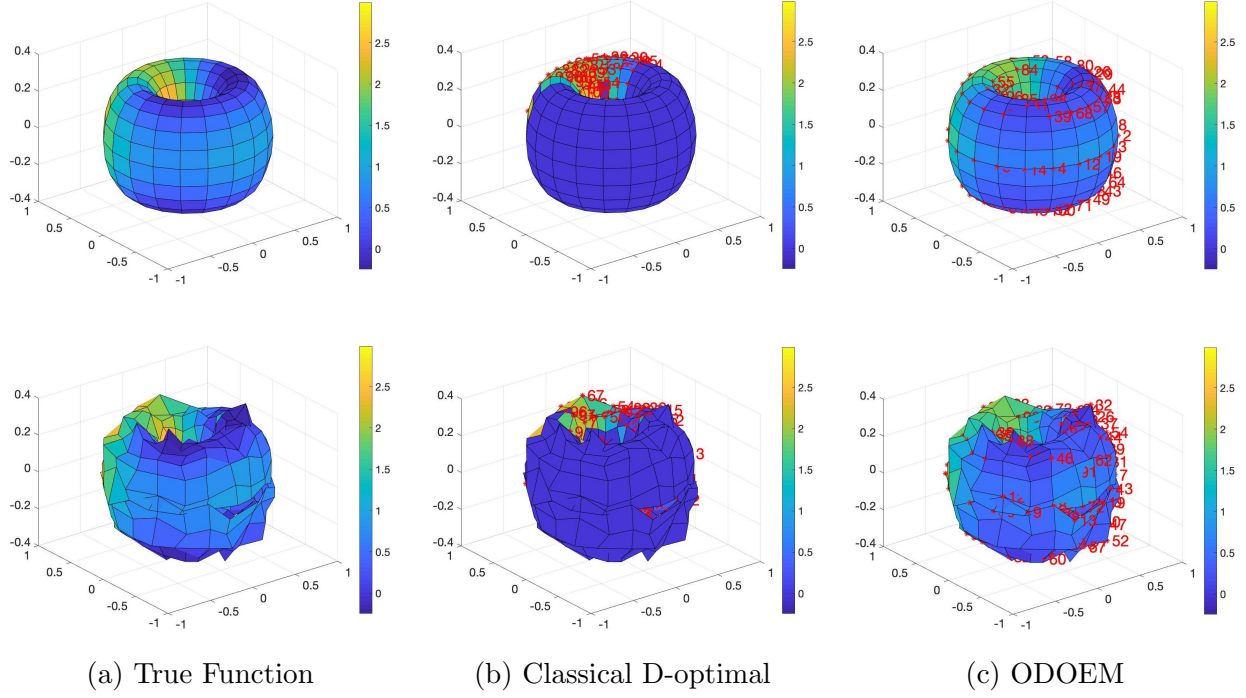


Figure 1: Torus example. Top: When $\{x_i\}_{i=1}^n$ lie on a Torus. Bottom: When $\{x_i\}_{i=1}^n$ are not exactly on a Torus. (a) The colors represent the true response values defined on the Torus. (b) 100 labeled instances (red numbers) and fitted response values (colors) by kernel regression D-optimal Design. (c) 100 labeled instances (red numbers) and fitted response values (colors) by ODOEM. As it can be seen here and in Figures 2-4, the predictions (c) approximate the true function on the manifold (a) well even if the data are observed with noise large enough that it distorts the observed manifold with respect to the original one.

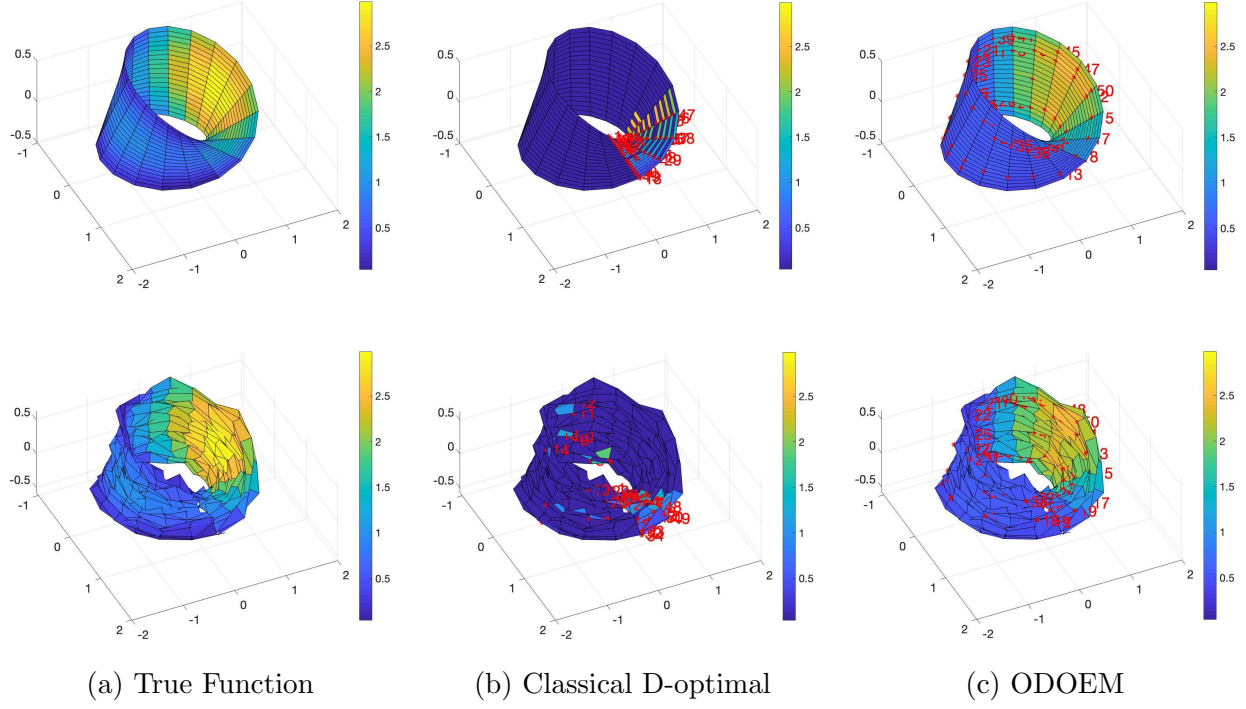


Figure 2: Möbius Strip. Top: When $\{x_i\}_{i=1}^n$ lie on a Möbius Strip. Bottom: When $\{x_i\}_{i=1}^n$ are not exactly on a Möbius Strip. (a) The colors represent the true response values defined on the Möbius Strip. (b) 100 labeled instances (red numbers) and fitted response values by kernel regression D-optimal Design. (c) 100 labeled instances (red numbers) and fitted response values (colors) by ODOEM.

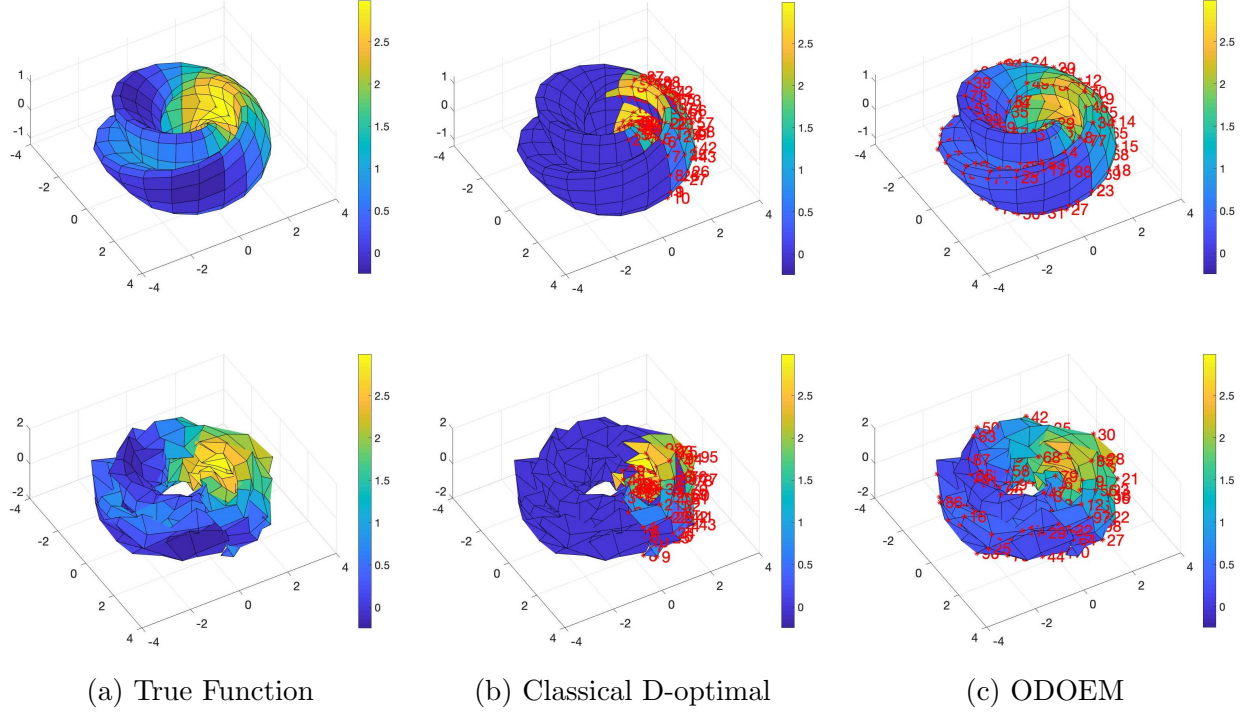


Figure 3: Figure “8” Immersion of Klein Bottle example. Top: When $\{x_i\}_{i=1}^n$ lie on a Figure “8” Immersion. Bottom: When $\{x_i\}_{i=1}^n$ are not exactly on a Figure “8” Immersion. (a) The colors represent the true response values defined on the Figure “8” Immersion. (b) 100 labeled instances (red numbers) and fitted response values (colors) by kernel regression D-optimal Design. (c) 100 labeled instances (red numbers) and fitted response values (colors) by ODOEM.

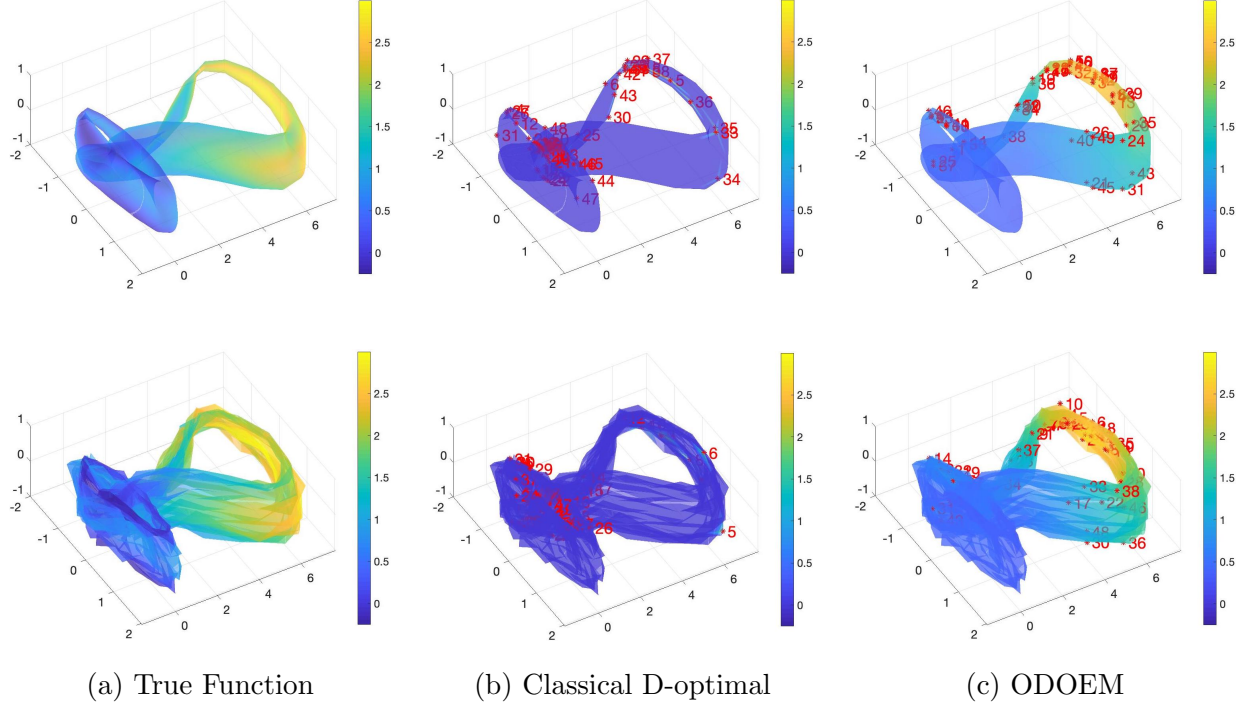


Figure 4: Bottle Shape of Klein Bottle example. Top: When $\{x_i\}_{i=1}^n$ lie on a Bottle. Bottom: When $\{x_i\}_{i=1}^n$ are not exactly on a Bottle. (a) The colors represent the true response values defined on the Bottle. (b) 100 labeled instances (red numbers) and fitted response values (colors) by kernel regression D-optimal Design. (c) 100 labeled instances (red numbers) and fitted response values (colors) by ODOEM.

5.2 Columbia Object Image Library

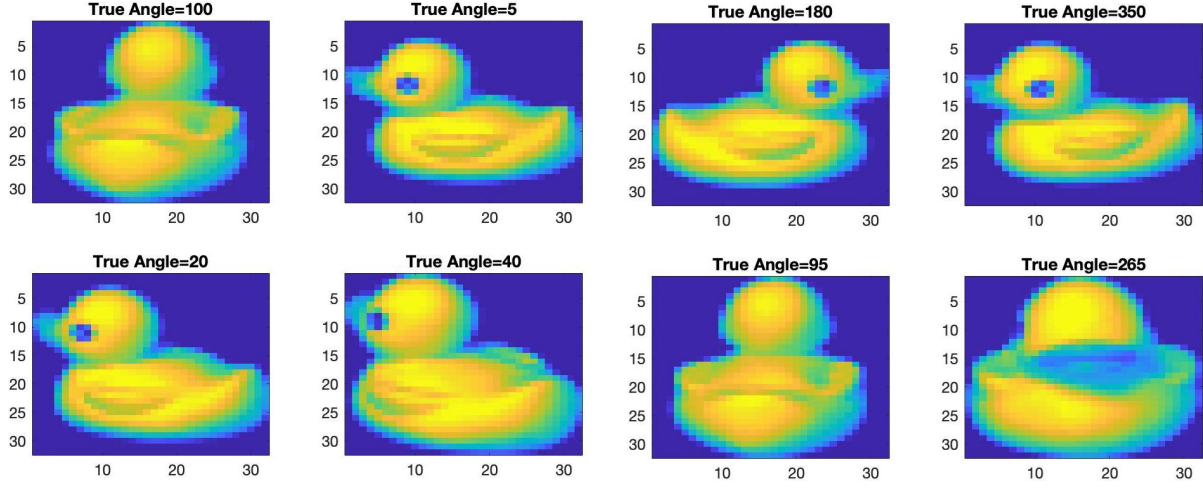
To demonstrate application to real-world datasets, we tested our ODOEM algorithm on the Columbia Object Image Library (**COIL-20**). COIL-20 is a database of grey-scale images of 20 different objects and these images were taken at pose intervals of 5 degrees for each object. There are two versions of this database. In this paper, we choose the processed database that contains 1440 32×32 normalized images.

In this set of experiments, the input data $\{x_i\}_{i=1}^n$ are the object images and the response values $\{y_i\}_{i=1}^n$ are the corresponding angles of these images. Given an object image, our goal is to estimate the angle of this object in the image. Among 20 different objects, we choose four different objects as illustration: a Rubber Duck, a Cannon, a Toy Car and a Piggy Bank. For each object, we apply the ODOEM algorithm to decide which instances to label and then train the LapRLS model (7) to predict the angles of the images using the labeled and unlabeled instances. Comparisons were made with the following alternative algorithms:

- Kernel regression model with a classical D-optimal Design;
- Kernel regression model with a random sampling scheme;
- Kernel regression model with a L_2 -discrepancy uniform design;
- Kernel regression model with a minimax uniform design;
- Kernel regression model with a maximin uniform design;
- SVM model with MAED (*Manifold Adaptive Experimental Design* Cai and He (2012));
- SVM model with TED (*Transductive Experimental Design*, Yu et al. (2008)).

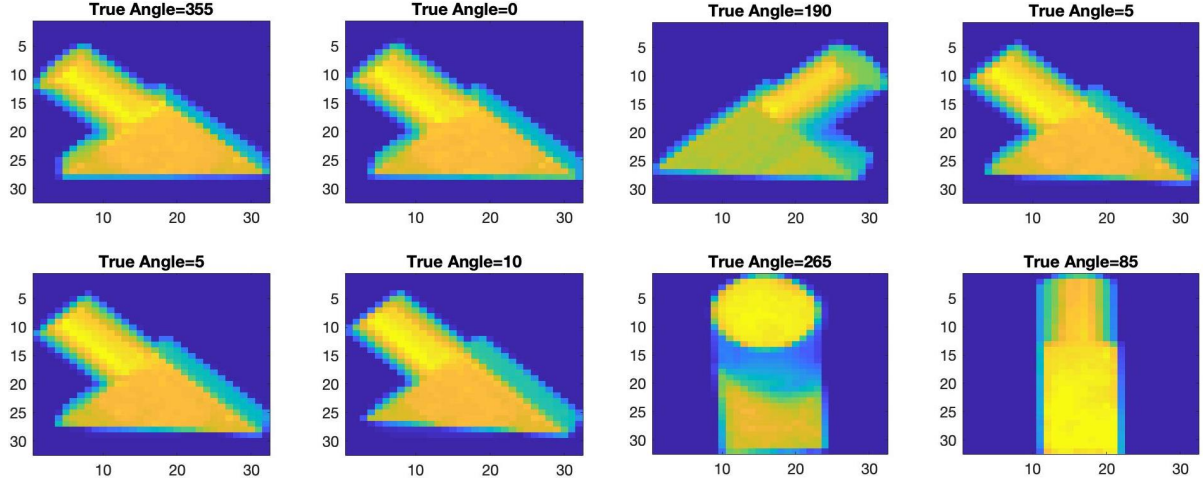
For both kernel regression and SVM, we used a RBF kernel and fixed the range parameter at 0.01. The results are shown in Figure 5-7. Figure 5-6 illustrate the first four images selected by classical D-optimal design and ODOEM for training the model. Figure 7 demonstrates the fitting performance (in terms of MSE) of different algorithms.

Based on the results, the following comments can be made: (a) Compared to the classical D-optimal design, there is a greater dispersion (in terms of angles) within the first four images selected by ODOEM, which improves the learning curve in Figure 7; (b) For some uniform design criteria, the corresponding optimization is not convex. Since the images are labeled sequentially, there is no guarantee that the global optimal can be achieved. This explains why some uniform designs do not work very well in these experiments. (c) MAED also benefits from incorporating the manifold structure into the design process. It leads to better fitting performance than other algorithms, except for ODOEM. (d) ODOEM outperforms all the other algorithms on all four object images.



(a) Classical D-optimal Design

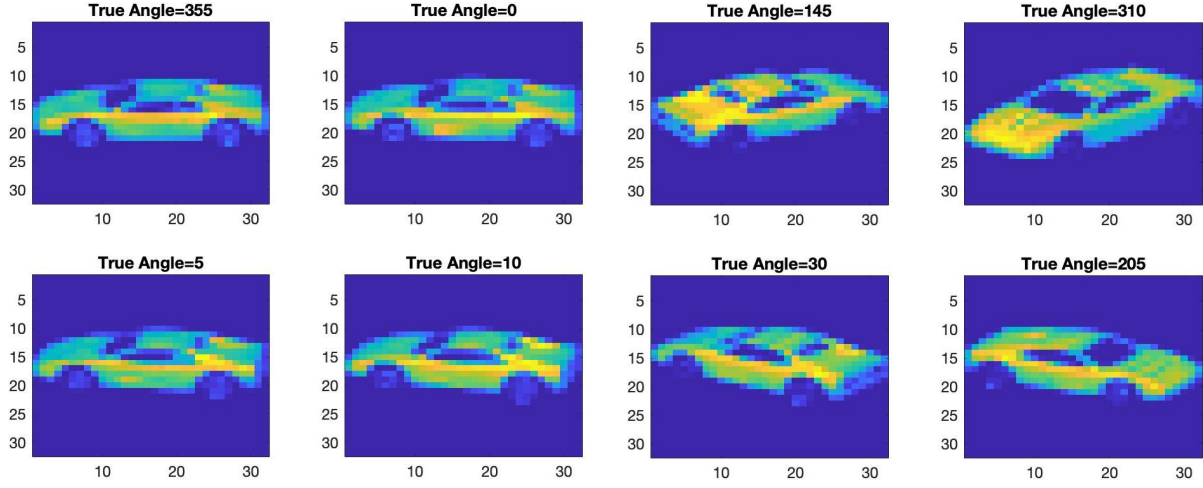
(b) ODOEM



(c) Classical D-optimal Design

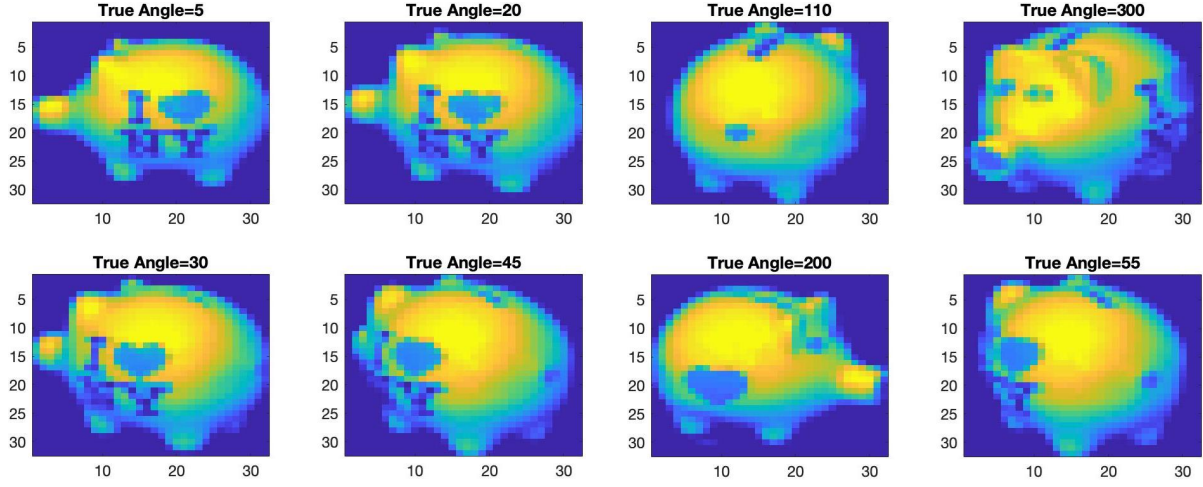
(d) ODOEM

Figure 5: Top: The first four Rubber Duck images selected by classical D-optimal design and ODOEM. Bottom: The first four Cannon images selected by classical D-optimal design and ODOEM. The true angle is labeled on top of each image.



(a) Classical D-optimal Design

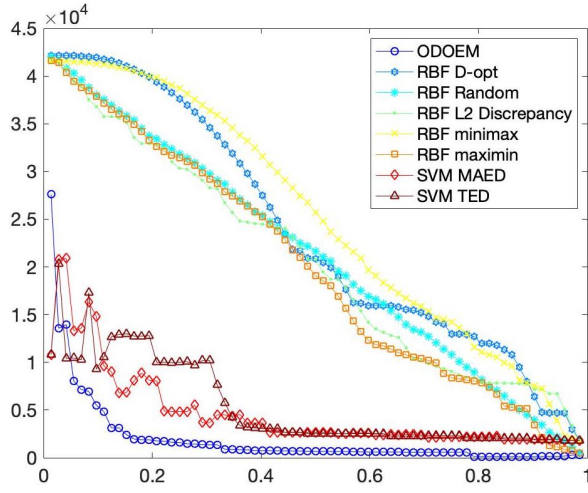
(b) ODOEM



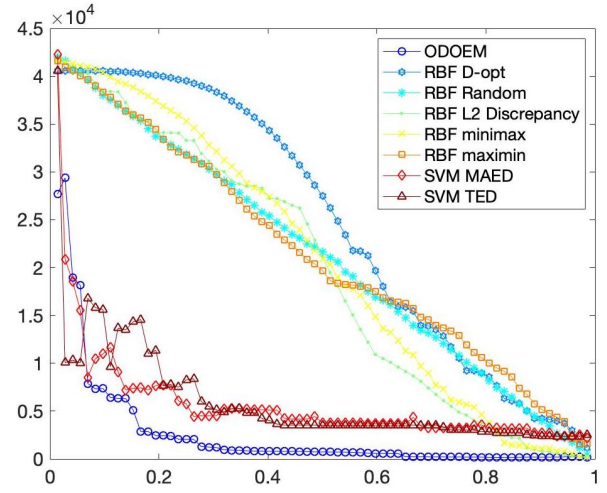
(c) Classical D-optimal Design

(d) ODOEM

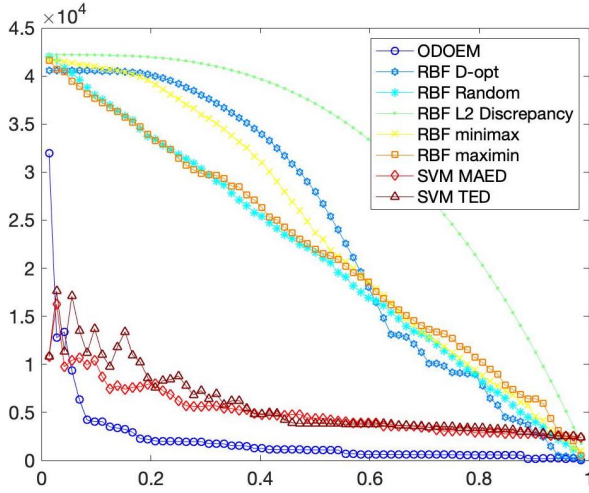
Figure 6: Top: The first four Toy Car images selected by classical D-optimal design and ODOEM.. Bottom: The first four Piggy Bank images selected by classical D-optimal design and ODOEM. The true angle is labeled on top of each image.



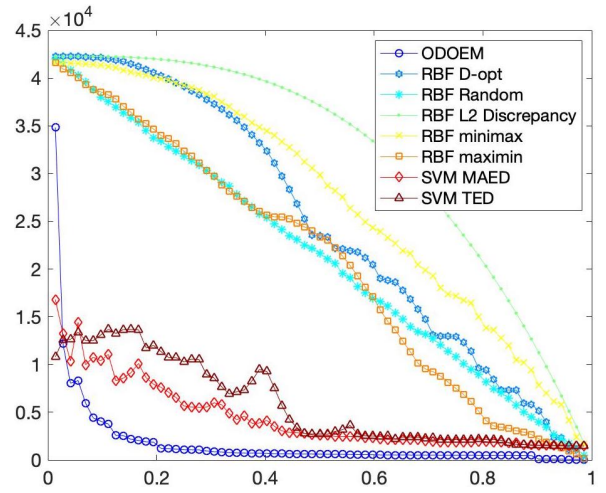
(a) Rubber Duck



(b) Cannon



(c) Toy Car



(d) Piggy Bank

Figure 7: MSE comparison among different algorithms on all four objects.

6 Conclusions

In this paper, we have developed a theoretical framework of optimal experimental designs on Riemannian manifolds. In particular, we have shown that D-optimal design and G-optimal design are equivalent on manifolds and have provided a new lower bound for the maximum prediction variance, demonstrating that this lower bound can be achieved at the D/G optimal design. In addition, we proposed a converging algorithm for the optimal design of experiments on manifolds. Finally we compared our proposing algorithm with other popular designs and models on several synthetic datasets and real-world image problems, and illustrated the competitive performance of our algorithm.

There are several directions of future research in this work. First, further research can be done to develop a systematic procedure for choosing the regularization parameters λ_A and λ_I . As discussed before, cross-validation is not a feasible strategy in a sequential learning problem since there are few or none labeled instances available at the beginning. Instead of using fixed values for regularization parameters, model selection criterion with theoretical justification might provide better learning performance. Similar work has been discussed by Li et al. (2019), where they maximize the likelihood function to choose the values of λ_A and λ_I in a Gaussian Process model. Secondly, there are other optimality criterion than the D/G “alphabetic” criteria in the field of optimal design of experiments. Under different optimal design criteria, new theoretical results of experimental design on manifolds can be explored. Thirdly, for very large scale problems with billions of discrete candidate points, evaluating each point with the corresponding design criteria is exhausting. Some modifications of our algorithm can be investigated, such as applying unsupervised clustering techniques first and then evaluate a representative point from each cluster.

References

- Alaeddini, A., E. Craft, R. Meka, and S. Martinez (2019). Sequential laplacian regularized v-optimal design of experiments for response surface modeling of expensive tests: An application in wind tunnel testing. *IISE Transactions*.
- Aronszajn, N. (1950). Theory of reproducing kernels. *Transactions of the American Mathematical Society* 68, 337–404.
- Belkin, M. (2003). *Problems of Learning on Manifolds*. Ph. D. thesis, The University of Chicago.
- Belkin, M. and P. Niyogi (2003). Laplacian eigenmaps for dimensionality reduction and data representation. *Neural Computation* 15(6), 1373–1396.
- Belkin, M. and P. Niyogi (2005). Towards a theoretical foundation for laplacian-based manifold methods. In *Proceedings of Conference on Learning Theory*.
- Belkin, M., P. Niyogi, and V. Sindhwani (2006). Manifold regularization: A geometric framework for learning from labeled and unlabeled examples. *Journal of Machine Learning Research* 7, 2399–2434.
- Box, G. and N. Draper (2007). *Response Surfaces, Mixtures, and Ridge Analyses*. Wiley Series in Probability and Statistics. Wiley.
- Box, G., J. Hunter, and W. Hunter (2005). *Statistics for experimenters: design, innovation, and discovery*. Wiley series in probability and statistics. Wiley-Interscience.
- Cai, D. and X. He (2012). Manifold adaptive experimental design for text categorization. *IEEE Transactions on Knowledge and Data Engineering* 24(4), 707–719.

- Chen, C., Z. Chen, J. Bu, C. Wang, L. Zhang, and C. Zhang (2010). G-optimal design with laplacian regularization. *Proceedings of the Twenty-Fourth AAAI Conference on Artificial Intelligence 1*, 413–418.
- Cheng, M. and H. Wu (2013). Local linear regression on manifolds and its geometric interpretation. *Journal of the American Statistical Association* 108(504), 1421–1434.
- Coifman, R., S. Lafon, A. Lee, M. Maggioni, B. Nadler, F. Warner, and S. Zucker (2005). Geometric diffusions as a tool for harmonic analysis and structure definition of data: Diffusion maps. *Proceedings of the National Academy of Sciences* 102(21), 7426–7431.
- Del Castillo, E. (2007). *Process optimization. A statistical approach*. Springer.
- Donoho, D. and C. Grimes (2003). Hessian eigenmaps: Locally linear embedding techniques for high dimensional data. *Proceedings of the National Academy of Sciences* 100(10), 5591–5596.
- Ettinger, B., L. M. Sangalli, and S. Perotto (2016, 02). Spatial regression models over two-dimensional manifolds. *Biometrika* 103(1), 71–88.
- Fedorov, V. (1972). *Theory of Optimal Design of Experiments*. Academic Press.
- Fedorov, V. V. (1972). *Theory of Optimal Experiments*. Academic Press.
- He, X. (2010). Laplacian regularized d-optimal design for active learning and its application to image retrieval. *IEEE Transactions on Image Processing* 19(1), 254–263.
- Hein, M., J. Y. Audibert, and U. von Luxburg (2005). From graphs to manifolds-weak and strong pointwise consistency of graph laplacians. In *Proceedings of the 18th Conference on Learning Theory*.

- Kiefer, J. (1974). General equivalence theory for optimum designs (approximate theory). *The Annals of Statistics* 2(5), 849–879.
- Kiefer, J. and J. Wolfowitz (1960). The equivalence of two extremum problems. *Canadian Journal of Mathematics* 12, 363–366.
- Lafon, S. (2004). *Diffusion Maps and Geometric Harmonics*. Ph. D. thesis, Yale University.
- Li, H., E. D. Castillo, and G. Runger (2019). On active learning methods for manifold data. *TEST*.
- Lin, L., B. S. Thomas, H. Zhu, and D. B. Dunson (2017). Extrinsic local regression on manifold-valued data. *Journal of the American Statistical Association* 112(519), 1261–1273.
- Marzio, M. D., A. Panzera, and C. C. Taylor (2014). Nonparametric regression for spherical data. *Journal of the American Statistical Association* 109(506), 748–763.
- Roweis, S. T. and L. K. Saul (2000). Nonlinear dimensionality reduction by locally linear embedding. *SCIENCE* 290, 2323–2326.
- Tenenbaum, J. B., V. de Silva, and J. C. Langford (2000). A global geometric framework for nonlinear dimensionality reduction. *Science* 290, 2319–2323.
- Vuchkov, I. (1977). A ridge-type procedure for design of experiments. *Biometrika* 64(2), 147–150.
- Wahba, G. (1990). *Spline models for observational data*. Philadelphia, PA: Society for Industrial and Applied Mathematics.

Yu, K., S. Zhu, W. Xu, and Y. Gong (2008). Non-greedy active learning for text categorization using convex transductive experimental design. *Proceedings of the 31st annual international ACM SIGIR conference on Research and development in information retrieval*, 635–642.

Appendix

Equation (12) Proof

Let $A = (Z_k^\top Z_k + \lambda_A I_p + \lambda_I X^\top L X)^{-1}$. Then:

$$\begin{aligned} AX^\top (XAX^\top)^{-1} XZ^\top \mathbf{y} &= (Z^\top X)^{-1} Z^\top XAX^\top (XAX^\top)^{-1} XZ^\top \mathbf{y} \\ &= (Z^\top X)^{-1} Z^\top XZ^\top \mathbf{y} \\ &= Z^\top \mathbf{y} \end{aligned}$$

Thus, we have

$$X^\top (XAX^\top)^{-1} XZ^\top \mathbf{y} = A^{-1} Z^\top \mathbf{y}$$

and therefore equation (10) can be reduced to equation (12). ■

Proposition 1 Proof

$$\begin{aligned} M_{Lap}(\epsilon_3) &= \int_{z \in \mathcal{X}} \xi_3(z) g(z) g(z)^\top dz + C \\ &= \int_{z \in \mathcal{X}} [(1 - \alpha) \xi_1(z) + \alpha \xi_2(z)] g(z) g(z)^\top dz + C \\ &= (1 - \alpha) \int_{z \in \mathcal{X}} \xi_1(z) g(z) g(z)^\top dz + (1 - \alpha) C + \alpha \int_{z \in \mathcal{X}} \xi_2(z) g(z) g(z)^\top dz + \alpha C \\ &= (1 - \alpha) M_{Lap}(\epsilon_1) + \alpha M_{Lap}(\epsilon_2) \end{aligned}$$
■

Proposition 2 Proof

Let M_{ij} be the (i, j) cofactor of the matrix $M_{Lap}(\epsilon_3)$ and let m_{ij} be the (i, j) element of the matrix $M_{Lap}(\epsilon_3)$. Then:

$$\begin{aligned}
\frac{d \log |M_{Lap}(\epsilon_3)|}{d\alpha} &= |M_{Lap}(\epsilon_3)|^{-1} \frac{d|M_{Lap}(\epsilon_3)|}{d\alpha} \\
&= |M_{Lap}(\epsilon_3)|^{-1} \sum_{i=1}^p \sum_{j=1}^p M_{ij} \frac{dm_{ij}(\alpha)}{d\alpha} \\
&= \sum_{i=1}^p \sum_{j=1}^p \left(M_{Lap}^{-1}(\epsilon_3) \right)_{ji} \left(\frac{dM_{Lap}(\alpha)}{d\alpha} \right)_{ij} \\
&= \text{Tr} \left(M_{Lap}^{-1}(\epsilon_3) \frac{dM_{Lap}(\alpha)}{d\alpha} \right) \\
&= \text{Tr} \left\{ M_{Lap}^{-1}(\epsilon_3) \frac{d[(1-\alpha)M_{Lap}(\epsilon_1) + \alpha M_{Lap}(\epsilon_2)]}{d\alpha} \right\} \\
&= \text{Tr} \left\{ M_{Lap}^{-1}(\epsilon_3) [M_{Lap}(\epsilon_2) - M_{Lap}(\epsilon_1)] \right\}
\end{aligned}$$

■

Proposition 3 Proof

1.

$$\begin{aligned}
&\int_{z \in \mathcal{X}} d(z, \epsilon) \xi(z) dz \\
&= \int_{z \in \mathcal{X}} g(z)^\top M_{Lap}^{-1}(\epsilon) g(z) \xi(z) dz \\
&= \int_{z \in \mathcal{X}} \text{Tr} \left\{ g(z)^\top M_{Lap}^{-1}(\epsilon) g(z) \right\} \xi(z) dz \\
&= p - \text{Tr} \left\{ M_{Lap}^{-1}(\epsilon) C \right\} \\
&= \int_{z \in \mathcal{X}} \text{Tr} \left\{ M_{Lap}^{-1}(\epsilon) [g(z)g(z)^\top + C - C] \right\} \xi(z) dz
\end{aligned}$$

$$\begin{aligned}
&= \int_{z \in \mathcal{X}} \text{Tr} \left\{ M_{Lap}^{-1}(\epsilon) [g(z)g(z)^\top + C] - M_{Lap}^{-1}(\epsilon)C \right\} \xi(z) dz \\
&= \int_{z \in \mathcal{X}} \left(\text{Tr} \left\{ M_{Lap}^{-1}(\epsilon) [g(z)g(z)^\top + C] \right\} - \text{Tr} \left\{ M_{Lap}^{-1}(\epsilon)C \right\} \right) \xi(z) dz \\
&= \text{Tr} \left\{ M_{Lap}^{-1}(\epsilon) \left[\int_{z \in \mathcal{X}} g(z)g(z)^\top \xi(z) dz + C \right] \right\} - \text{Tr} \left\{ M_{Lap}^{-1}(\epsilon)C \int_{z \in \mathcal{X}} \xi(z) dz \right\} \\
&= \text{Tr} \left\{ M_{Lap}^{-1}(\epsilon) \left[\int_{z \in \mathcal{X}} g(z)g(z)^\top \xi(z) dz + C \right] \right\} - \text{Tr} \left\{ M_{Lap}^{-1}(\epsilon)C \right\} \\
&= \text{Tr} \left\{ M_{Lap}^{-1}(\epsilon) M_{Lap}(\epsilon) \right\} - \text{Tr} \left\{ M_{Lap}^{-1}(\epsilon)C \right\} \\
&= p - \text{Tr} \left\{ M_{Lap}^{-1}(\epsilon)C \right\}
\end{aligned}$$

2. $\int_{z \in \mathcal{X}} d(z, \epsilon) \xi(z) dz = p - \text{Tr} \left\{ M_{Lap}^{-1}(\epsilon)C \right\}$ implies that $p - \text{Tr} \left\{ M_{Lap}^{-1}(\epsilon)C \right\}$ is the mean value of $d(z, \epsilon)$ for given design ϵ . Thus, we have

$$\max_{z \in \mathcal{X}} d(z, \epsilon) \geq p - \text{Tr} \left\{ M_{Lap}^{-1}(\epsilon)C \right\}$$

■

Proposition 4 Proof

Let ϵ_1 and ϵ_2 be two arbitrary designs on the experimental region \mathcal{X} and let $M_{Lap}(\epsilon_1)$ and $M_{Lap}(\epsilon_2)$ be the corresponding information matrices. Define the set of information matrices on \mathcal{X} as

$$M_{Lap}(\mathcal{X}) := \{M_{Lap}(\epsilon) | \epsilon \in \Xi\} \quad (69)$$

where Ξ is the set of all probability measure on \mathcal{X} . Clearly, $M_{Lap}(\epsilon_1), M_{Lap}(\epsilon_2) \in M_{Lap}(\mathcal{X})$. Based on Proposition 1, we have that

$$M_{Lap}(\epsilon_3) = (1 - \alpha)M_{Lap}(\epsilon_1) + \alpha M_{Lap}(\epsilon_2) \in M_{Lap}(\mathcal{X}) \quad (70)$$

where $M_{Lap}(\epsilon_3)$ is the information matrix for the design $\epsilon_3 = (1 - \alpha)\epsilon_1 + \alpha\epsilon_2$. This implies that $M_{Lap}(\mathcal{X})$ is a convex set.

In addition, in order to prove $\log |M_{Lap}(\epsilon)|$ is strictly concave, we also need to show that

$$\log |(1 - \alpha)M_{Lap}(\epsilon_1) + \alpha M_{Lap}(\epsilon_2)| > (1 - \alpha) \log |M_{Lap}(\epsilon_1)| + \alpha \log |M_{Lap}(\epsilon_2)| \quad (71)$$

for $\forall M_{Lap}(\epsilon_1) \neq M_{Lap}(\epsilon_2)$ and $\forall \alpha \in (0, 1)$. It is known that, for any positive-definite matrices A and B ,

$$|(1 - \alpha)A + \alpha B| \geq |A|^{1-\alpha} |B|^\alpha, \text{ where } \alpha \in (0, 1), \quad (72)$$

where the equality holds only if $A = B$. Since $M_{Lap}(\epsilon)$ is positive-definite, we have that

$$|(1 - \alpha)M_{Lap}(\epsilon_1) + \alpha M_{Lap}(\epsilon_2)| > |M_{Lap}(\epsilon_1)|^{1-\alpha} |M_{Lap}(\epsilon_2)|^\alpha. \quad (73)$$

Therefore,

$$\log |(1 - \alpha)M_{Lap}(\epsilon_1) + \alpha M_{Lap}(\epsilon_2)| > (1 - \alpha) \log |M_{Lap}(\epsilon_1)| + \alpha \log |M_{Lap}(\epsilon_2)|$$

■

Proposition 5 Proof

Based on Proposition 1, we have

$$\begin{aligned} M_{Lap}(\epsilon_{k+1}) &= (1 - \alpha)M_{Lap}(\epsilon_k) + \alpha M_{Lap}(\epsilon(z)) \\ &= (1 - \alpha)M_{Lap}(\epsilon_k) + \alpha(g(z)g(z)^\top + C) \\ &= (1 - \alpha) \left[M_{Lap}(\epsilon_k) + \frac{\alpha}{1 - \alpha} g(z)g(z)^\top + \frac{\alpha}{1 - \alpha} C \right] \end{aligned}$$

Then

$$\begin{aligned} &|M_{Lap}(\epsilon_{k+1})| \\ &= (1 - \alpha)^p \left| M_{Lap}(\epsilon_k) \left(I_p + \frac{\alpha}{1 - \alpha} M_{Lap}(\epsilon_k)^{-1} g(z)g(z)^\top + \frac{\alpha}{1 - \alpha} M_{Lap}(\epsilon_k)^{-1} C \right) \right| \\ &= (1 - \alpha)^p \left| M_{Lap}(\epsilon_k) \right| \left| I_p + \frac{\alpha}{1 - \alpha} M_{Lap}(\epsilon_k)^{-1} g(z)g(z)^\top + \frac{\alpha}{1 - \alpha} M_{Lap}(\epsilon_k)^{-1} C \right| \end{aligned}$$

Assume α is an infinitesimal number. It's known that

$$\begin{aligned}
& \left| I_p + \frac{\alpha}{1-\alpha} M_{Lap}(\epsilon_k)^{-1} g(z) g(z)^\top + \frac{\alpha}{1-\alpha} M_{Lap}(\epsilon_k)^{-1} C \right| \\
&= 1 + \frac{\alpha}{1-\alpha} \text{Tr}(M_{Lap}(\epsilon_k)^{-1} g(z) g(z)^\top + M_{Lap}(\epsilon_k)^{-1} C) \\
&= 1 + \frac{\alpha}{1-\alpha} d(z, \epsilon_k) + \frac{\alpha}{1-\alpha} \text{Tr}(M_{Lap}(\epsilon_k)^{-1} C)
\end{aligned}$$

Therefore, we have

$$|M_{Lap}(\epsilon_{k+1})| = (1-\alpha)^p \left| M_{Lap}(\epsilon_k) \right| \left[1 + \frac{\alpha}{1-\alpha} d(z, \epsilon_k) + \frac{\alpha}{1-\alpha} \text{Tr}(M_{Lap}(\epsilon_k)^{-1} C) \right]$$

■

Proposition 6 Proof

Based on Equation (43), $|M_{Lap}(\epsilon_{k+1})|$ is clearly an increasing function with respect to $d(z, \epsilon_k)$. In order to maximize the value of $\log |M_{Lap}(\epsilon_{k+1})|$, we choose $z_{k+1} = \underset{z \in \mathcal{X}}{\text{argmax}} d(z, \epsilon_k)$. Thus, we have that

$$\begin{aligned}
\log |M_{Lap}(\epsilon_{k+1})| &= p \log(1-\alpha) + \log |M_{Lap}(\epsilon_k)| \\
&\quad + \log \left[1 + \frac{\alpha}{1-\alpha} d(z_{k+1}, \epsilon_k) + \frac{\alpha}{1-\alpha} \text{Tr}(M_{Lap}(\epsilon_k)^{-1} C) \right].
\end{aligned}$$

It can be shown that

$$\begin{aligned}
& \frac{\partial \log |M_{Lap}(\epsilon_{k+1})|}{\partial \alpha} \\
&= \frac{d(z_{k+1}, \epsilon_k) - (p - \text{Tr}(M_{Lap}(\epsilon_k)^{-1} C)) + p\alpha(1 - d(z_{k+1}, \epsilon_k) - \text{Tr}(M_{Lap}(\epsilon_k)^{-1} C))}{(1-\alpha)[(1-\alpha) + \alpha d(z_{k+1}, \epsilon_k) + \alpha \text{Tr}(M_{Lap}(\epsilon_k)^{-1} C)]}.
\end{aligned}$$

Since

$$\frac{\partial \log |M_{Lap}(\epsilon_{k+1})|}{\partial \alpha} \geq 0,$$

then

$$d(z_{k+1}, \epsilon_k) - (p - \text{Tr}(M_{Lap}(\epsilon_k)^{-1} C)) + p\alpha(1 - d(z_{k+1}, \epsilon_k) - \text{Tr}(M_{Lap}(\epsilon_k)^{-1} C)) \geq 0.$$

After simplification, we have

$$\alpha \leq \frac{d(z_{k+1}, \epsilon_k) - (p - \text{Tr}(M_{Lap}(\epsilon_k)^{-1}C))}{p[d(z_{k+1}, \epsilon_k) - (1 - \text{Tr}(M_{Lap}(\epsilon_k)^{-1}C))]} \quad (74)$$

Clearly,

$$0 \leq \alpha \leq \frac{d(z_{k+1}, \epsilon_k) - (p - \text{Tr}(M_{Lap}(\epsilon_k)^{-1}C))}{p[d(z_{k+1}, \epsilon_k) - (1 - \text{Tr}(M_{Lap}(\epsilon_k)^{-1}C))]} \quad (75)$$

is the non-decreasing direction for the value of $\log |M_{Lap}(\epsilon_{k+1})|$. In addition, based on the Proposition 3 Equation (24), it is clear that

$$\frac{d(z_{k+1}, \epsilon_k) - (p - \text{Tr}(M_{Lap}(\epsilon_k)^{-1}C))}{p[d(z_{k+1}, \epsilon_k) - (1 - \text{Tr}(M_{Lap}(\epsilon_k)^{-1}C))]} \geq 0 \quad (76)$$

which guarantees the existence of α in Equation (75). Therefore, $\left\{ |M_{Lap}(\epsilon_k)| \right\}_k$ is a non-decreasing sequence. ■

Choice of λ_I

The regularization parameters λ_A and λ_I are usually selected by cross-validation. However, ODOEM is a sequential design algorithm and the order of labeled instance is important. The cross-validation idea of randomly dividing the labeled instances into training set and validation set does not work here. Thus, one can set fixed values for λ_A and λ_I . In our experiments, we set $\lambda_A = 0.01$ for numerical stability and generate a decreasing sequence of λ_I by setting $\lambda_I = -\ln(k/n)$, where k is the number of labeled instance at k -th iteration and n is the total number of instances. The reason we choose a decreasing sequence of λ_I comes from the penalized loss function (7) and the performance evaluation criterion $\text{MSE} = \sum_{i=1}^n (y_i - \hat{f}(z_i))^2$. For manifold regularization model, the estimated learning function \hat{f} is achieved by minimizing the objective function (7). At early iterations, there are

only few labeled instances, and \hat{f} would benefit more from penalizing the learning function along the manifold structure (second regularization term). As the number of labeled instances increase, larger λ_I might not lead to smaller MSE. For example, let's consider the extreme scenario when all the instances have been labeled, i.e. $k = n$. If one want to achieve smaller MSE = $\sum_{i=1}^n (y_i - \hat{f}(z_i))^2$, it is better to estimate \hat{f} by

$$\hat{f} = \underset{f \in \mathcal{H}_K}{\operatorname{argmin}} \sum_{i=1}^n (y_i - f(z_i))^2, \quad (77)$$

instead of using

$$\hat{f} = \underset{f \in \mathcal{H}_K}{\operatorname{argmin}} \sum_{i=1}^n (y_i - f(z_i))^2 + \lambda_A \|f\|_{\mathcal{H}_K}^2 + \lambda_I \mathbf{f}^\top L \mathbf{f}. \quad (78)$$

In summary, for a learning problem with a fixed number of labeled instances, λ_I can be chosen using cross-validation. For a learning problem with sequentially labeled instances, we set $\lambda_I = -\ln(k/n)$ so that we can get a decreasing sequence of λ_I as k increases and $\lambda_I = 0$ when all the instances have been labeled.